

On the Annual Cycle of Subsurface Heat Budget and Thermal Structure of the Tropical Atlantic¹⁾

Stefan Hastenrath

Department of Meteorology, University of Wisconsin, Madison

Jacques Merle

ORSTOM/LPDA, University of Paris VI

(Manuscript received 24.06.1986)

Abstract:

The annual march of thermal structure and heat budget of the upper hydrosphere in the tropical Atlantic is studied on the basis of subsurface soundings processed for two degrees latitude by four degrees longitude areas. The subsurface temperature conditions are strongly modulated by the annual cycle of the surface wind field, with extrema around April and August. Two major systems of annual variation stand out, namely, (i) a zonal seesaw in the equatorial belt, with a deepening of isothermal surfaces from April to August in the west and reverse changes in the east; and (ii) a northward migration of a belt of shallow mixed layer in the equatorial North Atlantic from around April to August. These changes in subsurface thermal structure also dominate the spatial pattern of annual cycle variations in oceanic heat storage. The bands of warmest surface waters and shallowest mixed-layer depth broadly coincide with the surface wind confluence and all three features are found farthest into the northern hemisphere at the height of the northern summer. By contrast, bands of thinnest and most intense thermocline are located around 2–4 °N and S symmetric to the Equator, and this hemispheric symmetry is best developed in the latter part of the northern winter semester, when the asymmetry in the surface wind field is weakest.

Zusammenfassung: Zum Jahrgang von Temperaturstruktur und Wärmehaushalt des tropischen Atlantik

Der Jahrgang von Temperaturstruktur und Wärmehaushalt des tropischen Atlantik wird auf Grund von in Blocks von zwei Breitengraden mal vier Längengraden zusammengefaßten Temperaturprofilmessungen untersucht. Die Temperaturverhältnisse der oberen Hydrosphäre werden in erheblichem Maße durch den Jahrgang des Oberflächenwindfeldes, mit Extremen um April und August, geprägt. Zwei Systeme jahreszeitlicher Änderungen sind besonders augenfällig, nämlich (i) ein zonales Schaukelsystem im äquatorialen Bereich, gekennzeichnet durch ein Tieferlegen isothermer Flächen vom April zum August im Westen und die umgekehrten Änderungen im Osten; und (ii) eine nordwärtige Verlagerung eines Gürtels von besonders seichter Sprungschicht im äquatorialen Nordatlantik von April bis August. Diese Veränderungen in der Temperaturstruktur der oberen Hydrosphäre bestimmen auch weitgehend die räumlichen Unterschiede im Jahrgang der ozeanischen Wärmespeicherung. Die Bänder mit wärmsten Oberflächengewässern und seichtester Mischungsschicht stimmen ungefähr mit der Lage der Konfluenz im Oberflächenwindfeld überein, wobei alle drei der vorgenannten Erscheinungen im Nordsommer am weitesten in die Nordhemisphäre verlagert anzutreffen sind. Demgegenüber finden sich Bänder von besonders dünner und intensiver Sprungschicht um 2–4 °N und S symmetrisch zum Äquator. Diese Symmetrie zwischen den Hemisphären ist am besten ausgeprägt gegen Ende des Nordwinterhalbjahres, wenn auch die Asymmetrie im Windfeld am schwächsten ist.

¹⁾ Dedicated to Professor H. Flohn on his 75th birthday.

Résumé: Sur le cycle annuel du bilan de chaleur sous la surface et de la structure thermique de l'atlantique tropical

On étudie la marche annuelle de la structure thermique et du bilan de chaleur de l'hydrosphère supérieure dans l'Atlantique tropical sur la base de sondages effectués sous la surface pour des aires s'étendant sur deux degrés de latitude et quatre degrés de longitude. Les conditions de température sous la surface sont largement modulées par le cycle annuel du vent en surface, avec des extrêmes vers avril et août. Deux systèmes principaux de variation annuelle se présentent (i) un basculement zonal dans la ceinture équatoriale avec creusement des surfaces isothermes à l'ouest d'avril à août et des changements inverses à l'est et (ii) une migration vers le nord, d'avril à août, d'une couche mélangée peu profonde s'étendant sur la partie équatoriale de l'Atlantique Nord. Ces changements dans la structure thermique sous la surface dominent également la configuration spatiale des variations annuelles de chaleur emmagasinée. Les bandes d'eaux de surface les plus chaudes et les couches les plus minces d'eaux mêlées coïncident, en gros, avec la confluence du vent de surface. Ces trois caractéristiques se trouvent le plus loin dans l'hémisphère nord lors de l'été boréal. Par opposition, des bandes à thermoclines très minces et les plus intenses se situent aux environs de 2 à 4 °N et S, symétriquement par rapport à l'équateur. Cette symétrie hémisphérique est la mieux réalisée dans la dernière partie du semestre d'hiver de l'hémisphère nord, lorsque l'asymétrie du champ de vent en surface est la plus faible.

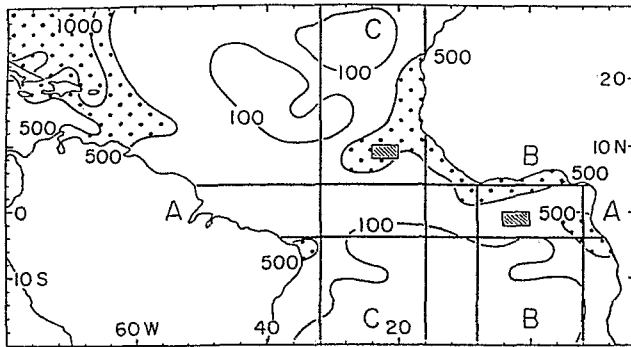
1 Introduction

More than ten years ago, we studied the surface atmospheric circulation and climate, sea surface temperature (SST) pattern, and surface hydrospheric heat budget in the tropical Atlantic from long-term surface ship observations (HASTENRATH and LAMB, 1977, 1978). While this work provided a comprehensive documentation of surface fields, it also indicated that an understanding of the annual cycle functioning of the combined atmosphere-ocean system would require the analysis of the subsurface temperature conditions. An extensive data bank of subsurface soundings in the tropical Atlantic has been compiled recently, and forms the basis for investigations into the subsurface thermal structure, oceanic heat budget, and annual cycle couplings of atmosphere and hydrosphere. The present note is a summary of interim findings.

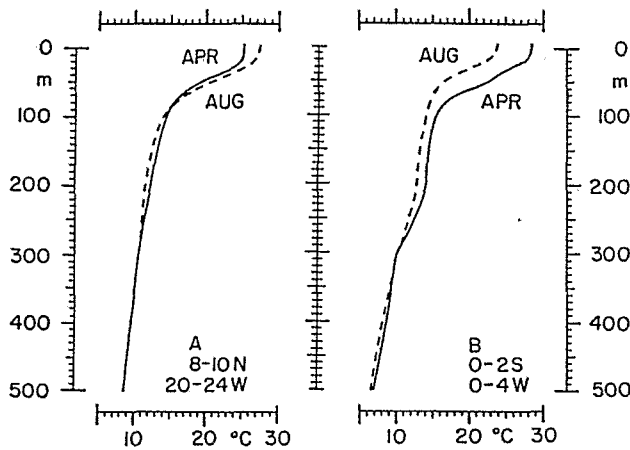
2 Observations and Basic Data Processing

This project utilizes both surface observations and subsurface temperature soundings. The collection of 1911–70 surface ship observations is described in HASTENRATH and LAMB (1977, 1978). For a detailed description of the subsurface data bank refer to MERLE and ARNAULT (1985) and HASTENRATH and MERLE (1986). Subsurface temperature soundings compiled until 1978 for the tropical Atlantic east of 80 °W and between 30 °N and 20 °S were combined into areas of 2 degrees latitude by 4 degrees longitude (ref. Figures 1 and 11), and by calendar month. Temperature data were processed for the depths of 0, 5, 10, 20, 30, 40, 50, 60, 75, 100, 125, 150, 200, 250, 300, 400, and 500 m. The uncertainty of average temperature values is estimated at less than 0.1 °C. The spatial distribution of soundings is also illustrated in Figure 1.

Mixed-layer depth (MIXLAY) is defined as the level at which temperature decreases to less than 1 °C below its surface value. This convention has been used previously in studies of the tropical oceans (WYRTKI, 1971; LAMB, 1984). LEVITUS (1982, p. 26–28) discusses various other criteria for application to different parts of the World ocean. The base of the thermocline is taken as the level from which downward the temperature decreases to less than 2 °C over a 50 m interval. This criterion was chosen from the inspection of numerous time-averaged temperature-depth profiles. In most of the study area throughout the year, the criterion captures the change from the sharp temperature contrasts across the thermocline to the layer of weak vertical temperature gradient below. An exception is the region poleward of about



● **Figure 1**
Orientation map showing breakdown into rectangles of 2 degrees latitude by 4 degrees longitude; number of soundings per rectangle (dot raster denotes areas with more than 500 soundings per rectangle); location of sample rectangles referred to in Figure 2; and location of zonal (A) and meridional (B and C) cross-sections in Figures 5–7.

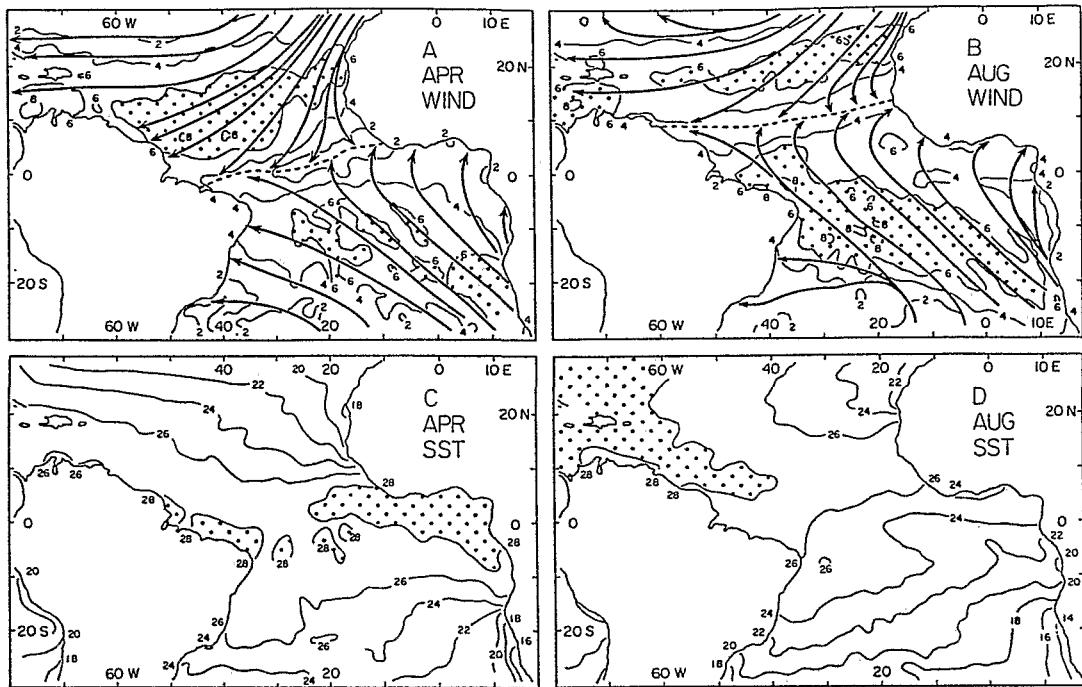


● **Figure 2**
Temperature-depth profiles in April (solid) and August (broken) in two sample rectangles: (a) 8–10 °N, 20–24 °W, and (b) 0–2 °S, 0–4 °W (ref. Figure 1).

20 °N during the northern winter half-year, when the base of the thermocline is ill-defined. Figure 2 exhibits the vertical temperature profiles during April and August in two sample rectangles (8–10 °N, 20–24 °W, and 0–2 °S, 0–4 °W; ref. Figure 1). These serve to illustrate the distinct development of the mixed layer and of the thermocline base. The vertical temperature gradient across the thermocline $\Delta T/\Delta Z$ is the temperature difference between top and base of thermocline divided by the thermocline thickness. The heat content of layers for all calendar months is calculated from the temperature at standard depths using the trapezoidal rule. Then the storage, or rate of change in heat content, is approximated by the difference of heat content of the following minus that of the preceding month divided by the time interval Δt of two months. The monthly subsurface heat storage Q_t , here evaluated to a depth of 500 m, is subtracted from the net surface heat gain ($Q_t + Q_v$), as presented in our atlas (HASTENRATH and LAMB, 1978), to yield an estimate of the divergence of heat transport within the ocean Q_v .

3 Surface Wind Field and Sea Surface Temperature Pattern

The annual cycle of the surface wind field and the SST pattern in the tropical Atlantic is fully documented in our atlas (HASTENRATH and LAMB, 1977, charts 14–25 and 50–61). Simplified maps for the extreme months April and August are presented in Figure 3. Only the most important features of the surface atmospheric circulation and of the SST pattern are summarized here.

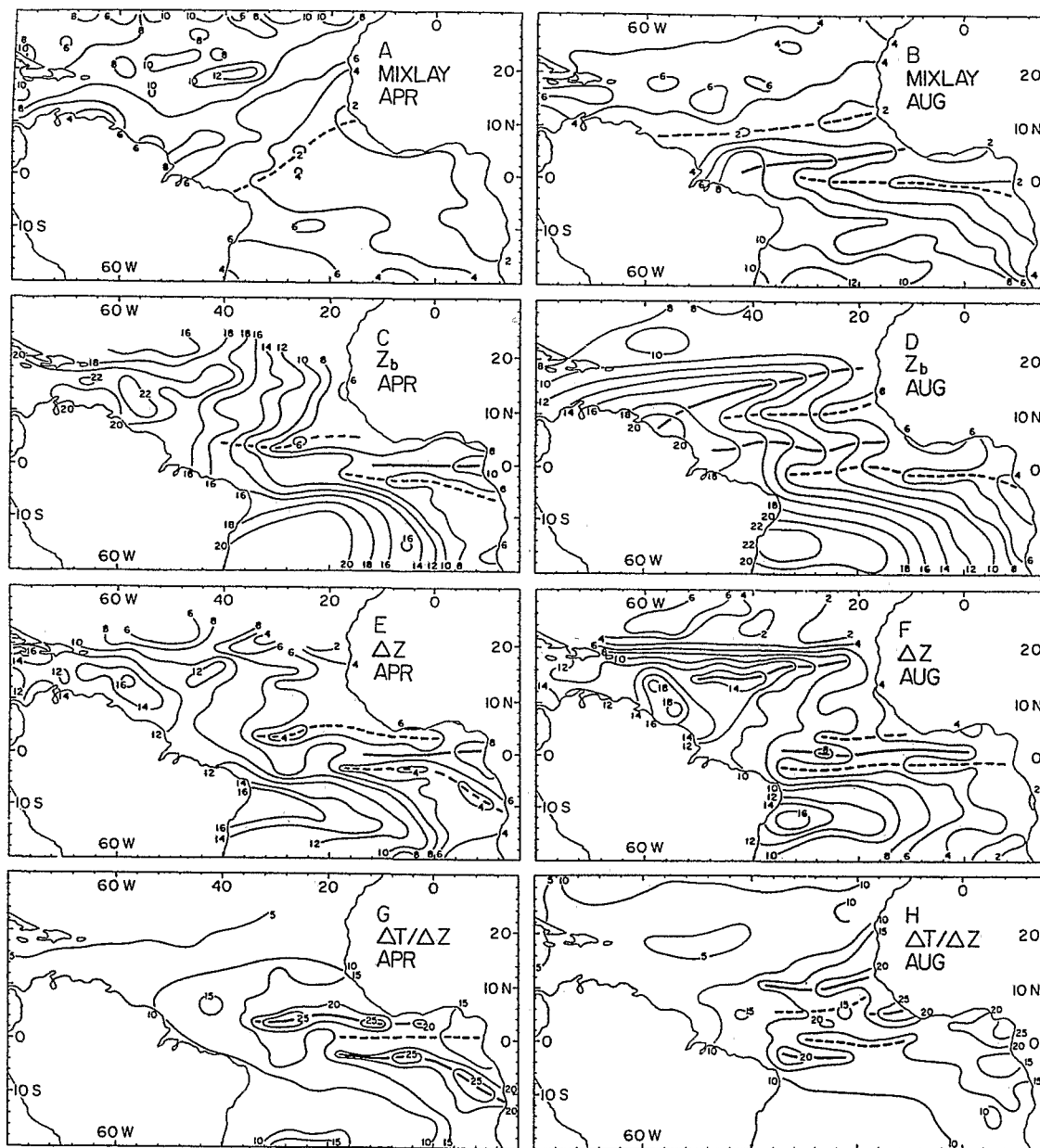


● **Figure 3** Climatic mean (1911–70) maps of surface resultant streamlines and isotachs (ms^{-1}) during (a) April and (b) August, and SST (in $^{\circ}\text{C}$) during (c) April and (d) August. Dot raster denotes, respectively, areas with wind speed larger than 6 ms^{-1} and SST larger than 28°C .

Throughout the year, the northeast trades and the cross-equatorial flow from the southern hemisphere meet in a confluence zone broadly embedded within a band of maximum SST to the north of the Equator. As the band of warmest surface waters, the aforementioned wind confluence reaches its southernmost location around March/April, and then migrates northward to attain a location farthest north at the height of the northern summer around August/September. At this extreme of the annual cycle, the cross-equatorial flow from the southern hemisphere exhibits over the eastern part of the ocean a marked clockwise curvature from southeasterly to southwesterly, with a prevailing southerly component in the equatorial region, while southeasterlies meet the northeast trades over the western Atlantic. At the height of the northern summer, the SST pattern is characterized by a far northerly position of a band of warmest waters in the tropical north Atlantic, contrasting with a tongue of cold water in the eastern Atlantic immediately to the south of the Equator. The southward shift of the band of warmest surface waters and of the associated wind confluence zone from around August/September to March/April is more gradual than the northward migration. Wind speed is highest in the core of the northeast and southeast trades.

4 Subsurface Thermal Structure

The subsurface temperature conditions in the tropical Atlantic have been analyzed by maps and cross-sections for all calendar months. These will be published in detail elsewhere. Only the charts of April and August are reproduced here, so as to illustrate conditions around the extrema of the annual cycle.



● Figure 4 Maps of subsurface thermal structure during April (left; a, c, e, g) and August (right; b, d, f, h).

(a, b) mixed-layer depth, MIXLAY, in tens of m;

(c, d) base of thermocline, Z_b , in tens of m;

(e, f) thermocline thickness, ΔZ , in tens of m;

(g, h) temperature gradient across the thermocline, in $10^{-2} \text{ }^\circ\text{C m}^{-1}$.

Heavy solid lines denote relative maxima, and heavy broken lines relative minima.

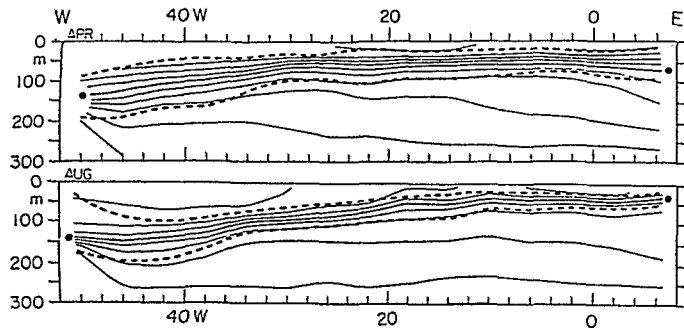
Figure 4 shows the April and August maps of mixed-layer depth, thermocline base, thermocline thickness, and temperature gradient across the thermocline. The mixed-layer depth in April (Figure 4a) is shallowest in a broad band extending from West Africa southwestward to Northeast Brazil, broadly coincident with the band of warmest surface waters (Figure 3c) embedded into which is the confluence zone of the surface wind field (Figure 3a). In August (Figure 4b), the zone of minimum mixed-layer depth is narrow and definite, and also extends from the African coast to the Americas, but is found at a more northerly latitude than in April (Figure 4a). Again, this band of minimum mixed-layer depth broadly coincides with the zone of maximum SST (Figure 3d) containing the confluence axis in the surface wind field (Figure 3b). Figure 4b furthermore shows a pronounced trough-ridge structure of mixed-layer depth, not apparent on the April chart (Figure 4a). Thus, to the south of the aforementioned band of shallowest mixed layer, a zone of relatively large values stretches, to the north of the Equator, from the mouth of the Amazon into the Gulf of Guinea, while immediately to the south of the Equator a tongue of shallow mixed-layer protrudes from the African coast into the Central Atlantic. The latter feature broadly coincides with the tongue of cold surface waters prominent in Figure 3d.

The base of the thermocline (Figures 4c, 4d) shows patterns similar, but not identical to those of mixed-layer depth (Figures 4a, 4b). Thus, in April a tongue of shallowest thermocline base protrudes from West Africa southwestward. However, a zone of relative maximum of depth of thermocline base extending in the equatorial region from the Gulf of Guinea to the Americas separates that zone of minimum thermocline base from another tongue of shallow thermocline base immediately to the south of the Equator in the eastern Atlantic. In August (Figure 4d), the northern hemispheric tongue of minimum thermocline base is shifted far northward, giving way to a zone of relative maximum immediately to the north of the Equator, while a tongue of shallowest thermocline base persists in the eastern Atlantic to the south of the Equator.

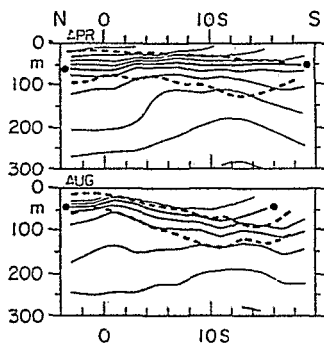
The vertical displacements of the thermocline in the course of the year do not occur en bloc, but are associated with changes in thickness and intensity of the thermocline, as illustrated in Figures 4e to 4h. The thermocline thickness in April (Figure 4e) is smallest in a broad tongue extending from West Africa westward, and in another tongue protruding to the south of the Equator from the African coast far into the open Atlantic. A corresponding trough and ridge structure is apparent on the April map of the vertical temperature gradient across the thermocline (Figure 4g), which shows a most intense thermocline in two well-defined narrow bands one to the north of the Equator, and the other in the eastern Atlantic immediately to the south of the Equator. Thus, in the regions with a shallow base, the thermocline tends to be thin and intense. The August map of thermocline thickness (Figure 4f) also shows considerable similarity to that of the thermocline base (Figure 4d), whereas the thermocline temperature gradient (Figure 4h) in August shows little tendency to be steepest in the regions of thinnest thermocline.

The selection of maps reproduced in Figures 4 and 3 illustrates that the patterns of mixed-layer depth and SST tend to be asymmetric with respect to the Equator, as is the surface wind field. Bands of warmest surface waters and shallowest mixed layer broadly coincide with the surface wind confluence and all three features are found farthest into the northern hemisphere at the height of the northern summer. By contrast, the bands of thinnest and most intense thermocline tend to be centered around 2–4 °N and S symmetric to the Equator. This hemispheric symmetry is best developed in the latter part of the northern winter semester, when the asymmetry of the surface wind field is weakest.

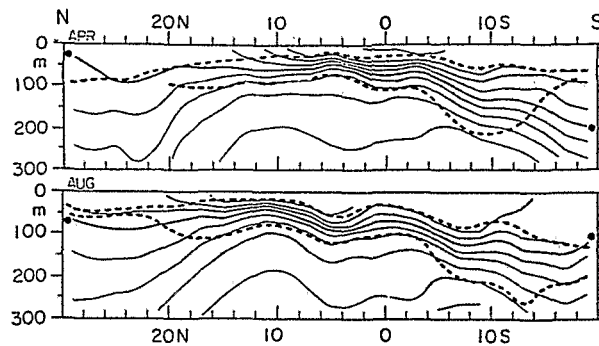
The subsurface thermal structure in the tropical Atlantic is further illustrated by zonal (Figure 5, profile A in Figure 1) and meridional (Figure 6, profile B in Figure 1; Figure 7, profile C in Figure 1) vertical cross-sections. The zonal transects along the Equator (Figure 5) show as most prominent changes from April to August a lowering of isothermal surfaces to the west and a rise to the east. Concomitantly, the thermocline thins over much of the transect. As the maps of Figure 4, and the meridional transects in Figures 6 and 7, the zonal cross-section Figure 5 illustrates that the thermocline does not rise and drop



● **Figure 5**
Zonal cross-sections along the Equator during April and August. See Figure 1 for location of profile A. Thick solid lines with heavy dots at extremities represent 20 °C isotherm, and thin solid lines other isotherms at 2 °C intervals. Heavy broken lines denote the depth of the mixed layer and the base of the thermocline.



● **Figure 6** Meridional cross-section across the Eastern Atlantic during April and August. See Figure 1 for location of profile B. Symbols as for Figures 5 and 7.



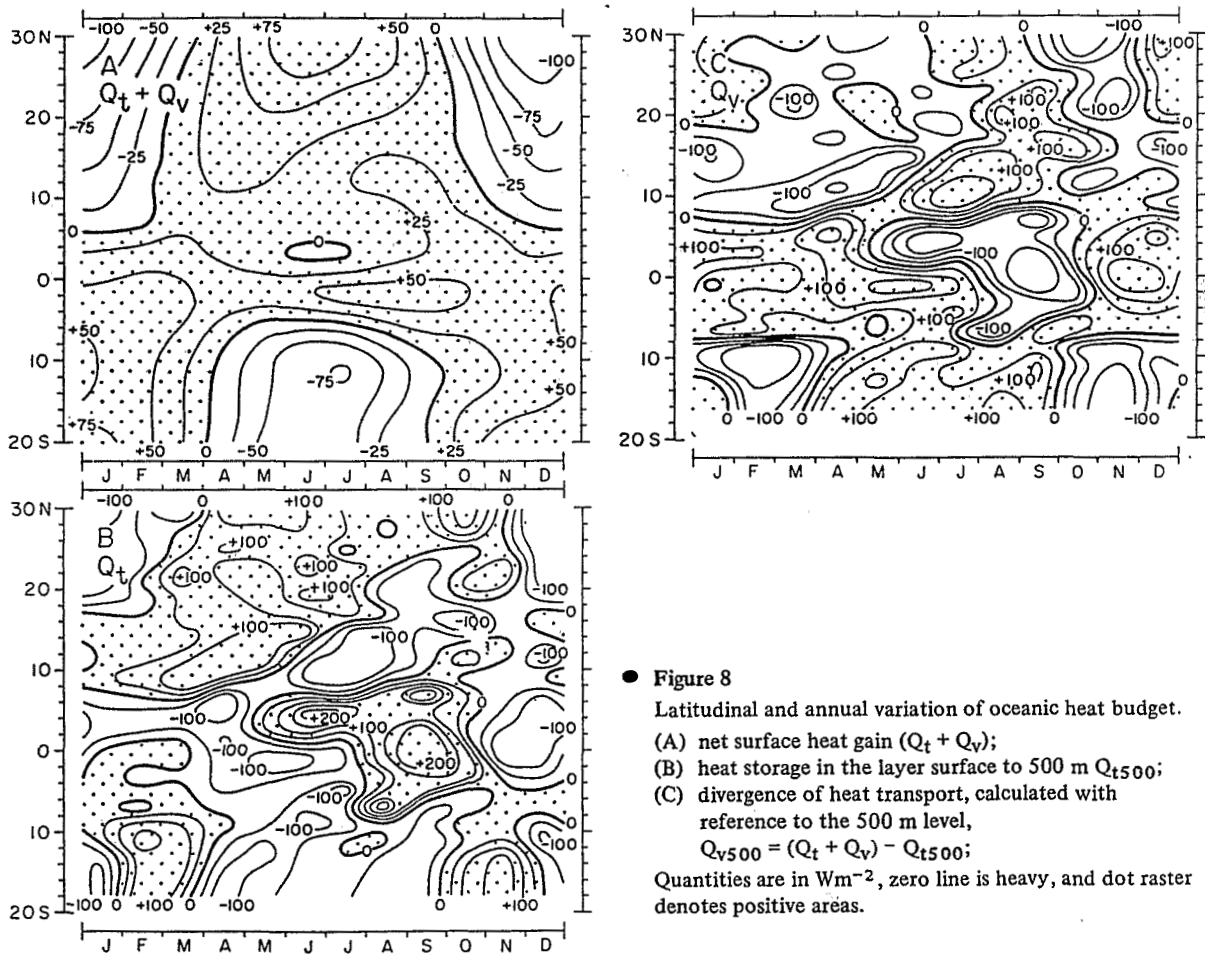
● **Figure 7** Meridional cross-sections across the Central Atlantic during April and August. See Figure 1 for location of profile C. Symbols as for Figures 5 and 6.

en bloc, but also undergoes structural changes in the course of the year. The meridional cross-section in the Eastern Atlantic (Figure 6) likewise exhibits substantial changes from April to August: In the equatorial region the thermocline rises and becomes thinner while it deepens substantially in the South Atlantic. The meridional cross-section across the Central Atlantic (Figure 7) encompasses the realm of the Intertropical Convergence Zone. As illustrated in Figures 3a, 3b, the surface wind confluence shifts from around 2 °N in April to 12 °N in August. The thermocline variations in this latitude domain are of particular interest. Proceeding from April to August, the latitude of shallowest mixed layer changes from around 5 °N to beyond 10 °N, while the mixed-layer and the base of the thermocline deepen in the band of about 0–7 °N. The role of these seasonal variations of subsurface thermal structure for the annual cycle functioning of the Intertropical Convergence Zone is currently being studied.

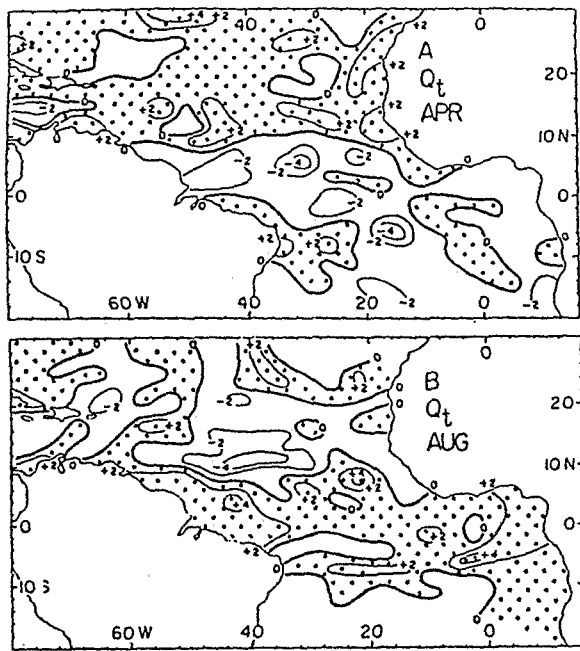
From the analysis of subsurface thermal structure two major systems of annual cycle changes stand out, namely (i) a seesaw in the zonal direction in the equatorial belt, and (ii) a meridional shift of patterns in the low-latitude North Atlantic. These also appear instrumental in the annual cycle of the oceanic heat budget.

5 Oceanic Heat Budget

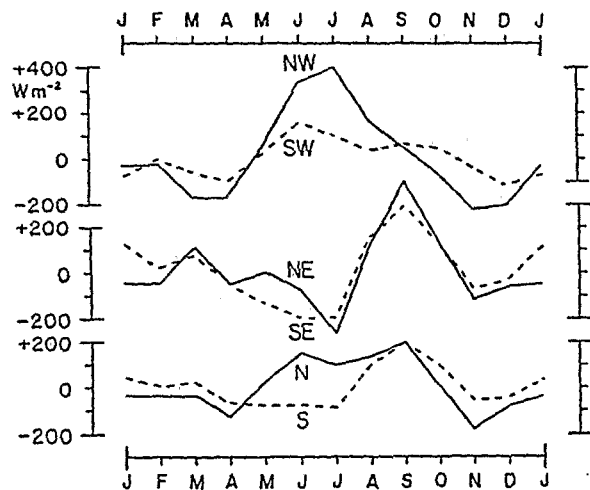
Three quantities related to the oceanic heat budget are to be considered in context: The net surface heat gain ($Q_t + Q_v$); the heat storage within the hydrospheric column Q_t ; and the divergence of the heat transport in the ocean Q_v , which is obtained as the difference between the former two quantities. Diagrams showing the latitudinal and annual variation of $(Q_t + Q_v)$, Q_t , and Q_v , are presented in Figure 8. The diagram of $(Q_t + Q_v)$ shows for the equatorial region a net surface heat gain throughout the year, while further away from the Equator heat gain/loss prevails in the respective summer/winter season. The panel of oceanic heat storage Q_t exhibits for the zones poleward of about 15°N and S heat storage/depletion predominating during the respective summer/winter half-years, while patterns are more complicated in the equatorial zone. In the band $0-6^\circ\text{N}$, heat depletion is largest around March/April, and storage around June-September. In the zone $0-6^\circ\text{S}$ extrema occur somewhat later. On the whole, the temporal and spatial variations of Q_t are much larger than those of $(Q_t + Q_v)$. Accordingly, the diagram of Q_v is complementary to that of Q_t . The panel of oceanic heat storage Q_t (Figure 8, part b) is broadly consistent with the latitude mean evaluation of LAMB and BUNKER (1982), but is less readily compared to LEVITUS (1984, Figure 14), who presents plots of heat content rather than of heat storage Q_t (i.e. rate of change in heat content).



● **Figure 8**
 Latitudinal and annual variation of oceanic heat budget.
 (A) net surface heat gain ($Q_t + Q_v$);
 (B) heat storage in the layer surface to 500 m Q_{t500} ;
 (C) divergence of heat transport, calculated with
 reference to the 500 m level,
 $Q_{v500} = (Q_t + Q_v) - Q_{t500}$;
 Quantities are in Wm^{-2} , zero line is heavy, and dot raster
 denotes positive areas.



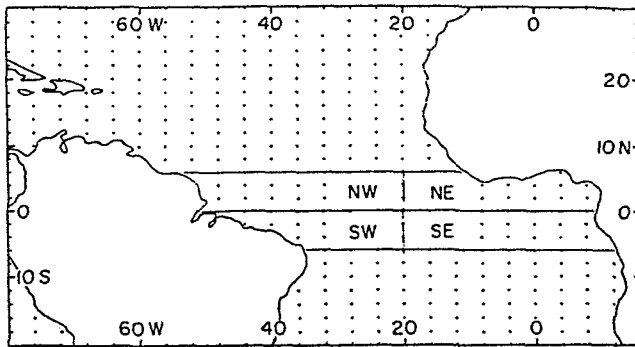
● Figure 9
Maps of heat storage in the layer surface to 500 m, Q_{t500} in (a) April and (b) August, in 10^2 Wm^{-2} . Zero line is heavy, and dot raster denotes positive areas.



● Figure 10
Annual march of subsurface heat storage (Q_t) in the layer surface to 500 m in the equatorial Atlantic, in Wm^{-2} . See Figure 11 for delineation of areas.
NW, solid line: $0-6^\circ \text{N}$, West of 20°W ;
SW, broken line: $0-6^\circ \text{S}$, West of 20°W ;
NE, solid line: $0-6^\circ \text{N}$, East of 20°W ;
SE, broken line: $0-6^\circ \text{S}$, East of 20°W ;
N, solid line: $0-6^\circ \text{N}$, zonal average;
S, broken line: $0-6^\circ \text{S}$, zonal average.

The April and August maps of Q_t in Figure 9 serve to illustrate the two major systems of annual cycle variations of the oceanic heat budget in the low-latitude Atlantic.

(i) In the equatorial belt, a seesaw in the zonal direction is apparent, in such a way that in the west the isothermal surfaces rise and the hydrospheric heat content decreases around April, whereas in August the isothermal surfaces are depressed and positive heat storage takes place. This tendency for broadly inverse variations of oceanic heat content between the western and eastern portions of the equatorial Atlantic is further illustrated in Figures 10 and 11.



● **Figure 11**
Orientation map showing boxes referred to in Figure 10, as well as breakdown into rectangles of 2 degrees latitude by 4 degrees longitude.

(ii) In the equatorial North Atlantic, a band of heat depletion (negative Q_t) shifts northward from around April to August, giving way to heat storage (positive Q_t) in the zone immediately to the North of the Equator. This system of variations in oceanic heat content accompanies the latitudinal migration of a zone of shallowest mixed layer, which in turn is associated with a band of warmest surface waters and the confluence in the surface wind field.

6 Concluding Remarks

An improved data bank of oceanic soundings allowed a preliminary analysis of spatial patterns and annual cycle of subsurface thermal structure and heat budget in the tropical Atlantic. The most prominent systems of annual cycle variations include (i) a zonal seesaw of the equatorial belt, with a lowering of isothermal surfaces from around April to August in the west and the reverse changes in the east; (ii) a seasonal latitude migration of a band of shallow mixed-layer concomitant with a zone of warmest surface waters and wind confluence zone, with a position closest to the Equator around April and a northernmost location around August. These systems in subsurface thermal structure also dominate the annual march of oceanic heat content in the low-latitude Atlantic. The patterns of SST and mixed-layer depth are asymmetric with respect to the Equator most markedly at the height of the northern summer, when the asymmetry in the surface wind field is most pronounced. Contrariwise, bands of thinnest and most intense thermocline are located symmetric to the Equator around 2–4 °N and S, and this hemispheric symmetry is best developed in the latter part of the northern winter semester, when the asymmetry of the surface wind field is weakest. Major topics of ongoing work include the role of Ekman pumping in the seasonal changes of the subsurface thermal structure, and in particular the amphibious nature of the Intertropical Convergence Zone of the low-latitude Atlantic.

Acknowledgements

S.H. acknowledges support through U.S. National Science Foundation Grant OCE85-15009, and J.M. support by the Programme National d'Étude de la Dynamique du Climat through the FOCAL (Français Océan Climat Atlantique Équatorial) Experiment. Carol EVANS and Eric HACKERT did the computer programming at the University of Wisconsin.

References

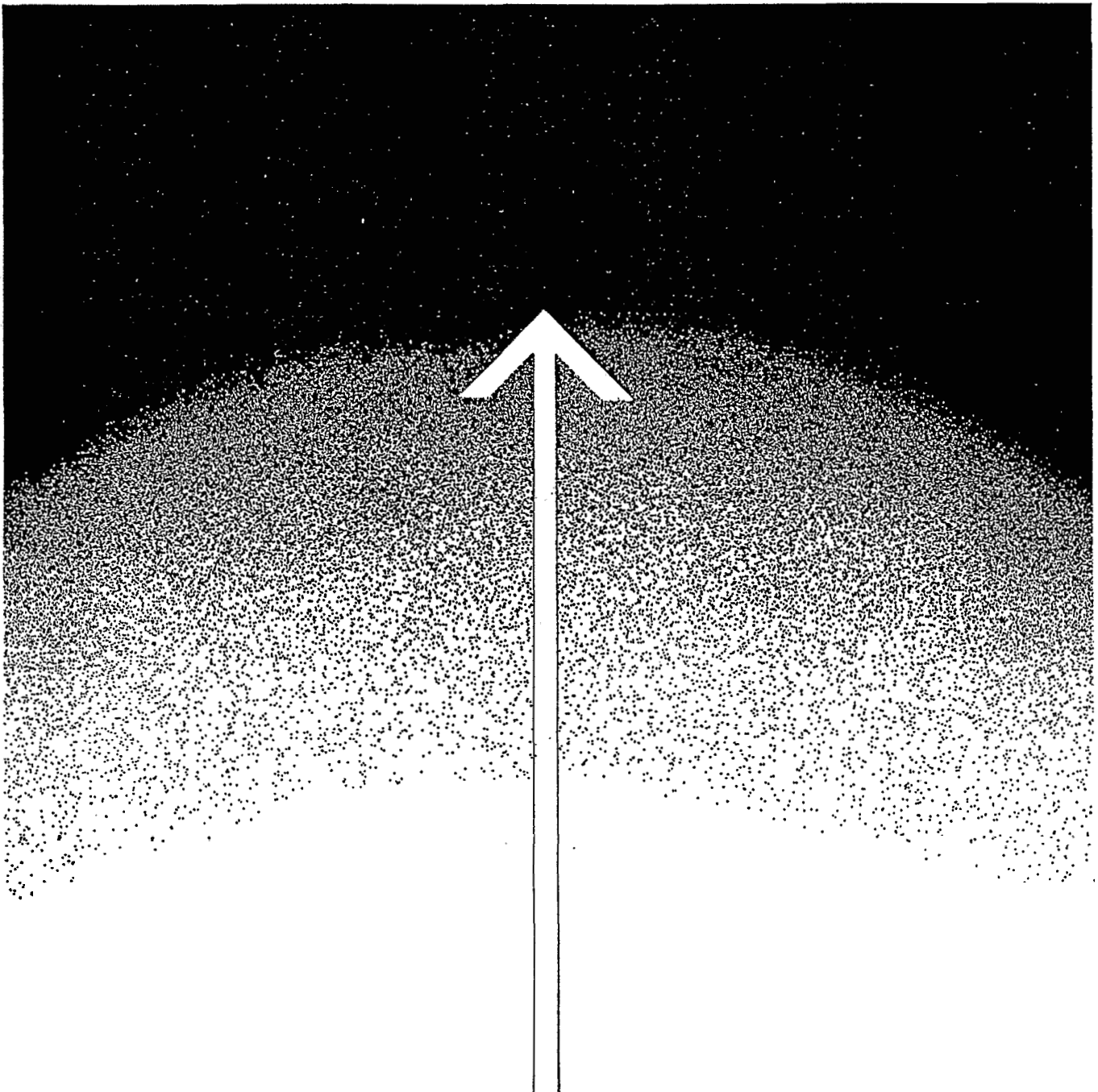
- HASTENRATH, S. and P. LAMB, 1977: Climatic atlas of the tropical Atlantic and Eastern Pacific Oceans. University of Wisconsin Press, Madison, 112 pp.
- HASTENRATH, S. and P. LAMB, 1978: Heat budget atlas of the tropical Atlantic and Eastern Pacific Oceans. University of Wisconsin Press, Madison, 104 pp.
- HASTENRATH, S. and J. MERLE, 1986: On the annual march of heat storage and export in the tropical Atlantic Ocean. *J. Phys. Oceanogr.* 16, 694–708.
- LAMB, P., 1984: On the mixed-layer climatology of the North and tropical Atlantic. *Tellus* 36A, 292–305.
- LAMB, P. and A. F. BUNKER, 1982: The annual march of the heat budget of the North and tropical Atlantic Oceans. *J. Phys. Oceanogr.* 12, 1388–1410.
- LEVITUS, S., 1982: Climatological atlas of the World ocean. NOAA Professional Paper No. 13, Rockville, Md., 173 pp.
- LEVITUS, S., 1984: Annual cycle of temperature and heat storage in the World ocean. *J. Phys. Oceanogr.* 14, 727–746.
- MERLE, J. and S. ARNAULT, 1985: Seasonal variability of the surface dynamic topography in the tropical Atlantic Ocean. *J. Mar. Res.* 43, 267–288.
- WYRTKI, K., 1971: Oceanographic atlas of the International Indian Ocean Expedition. National Science Foundation, Washington, D.C., 531 pp.

Reprint

Contributions to
Atmospheric Physics

Beiträge zur
Physik der Atmosphäre

Vieweg



11 MARS 1996

ORSTOM Documentation



010001208

O.R.S.T.O.M. Fonds Documentaire

N° : 43854

Cote : B ex 1